A Direct Search for Dirac Magnetic Monopoles

The CDF Collaboration
URL http://www-cdf.fnal.gov
(Dated: August 11, 2004)

Magnetic monopoles are highly ionizing and curve in the direction of the magnetic field. A new dedicated magnetic monopole trigger at CDF, which requires large pulses in the time-of-flight scintillators, remains highly efficient to monopoles while consuming a tiny fraction of the available bandwidth. A specialized offline reconstruction checks the central drift chamber for large dE/dx tracks which do not curve in the plane perpendicular to the magnetic field. We observed zero monopole candidate events in 35.7 pb^{-1} of proton-antiproton collisions at $\sqrt{s} = 1.96$ TeV. This implies a monopole production cross section limit $\sigma < 0.3$ pb for monopoles with mass between 100 and 700 GeV, and, for a Drell-Yan like pair production mechanism, a mass limit $m > 350$ GeV.

I. INTRODUCTION

The existence of magnetic monopoles would add symmetry to Maxwell's equations without breaking any known physical law. More dramatically, it would make charge quantization a consequence of angular momentum quantization, as first shown by Dirac [1]. With such appeal, monopoles continue to excite interest and new searches despite their elusiveness to date.

Grand unified theories predict monopole masses of about 10^{17} TeV, so there have been extensive searches for high mass monopoles produced by cosmic rays [2]. Indirect searches for low mass monopoles have looked for the effects of virtual monopole/anti-monopole loops added to QED Feynman diagrams [3]. Detector materials exposed to radiation from $p\bar{p}$ collisions at the Tevatron have been examined for trapped monopoles [4]. All results have been negative [5].

In this article, we describe a search for Dirac monopoles with mass less than 1 TeV. By a "Dirac" monopole, we mean a particle bearing no electric charge, having no hadronic interactions, and whose magnetic charge g satisfies the Dirac quantization condition:

$$\frac{ge}{\hbar c} = \frac{n}{2} \Longleftrightarrow \frac{g}{e} = \frac{n}{2\alpha} \approx 68.5 \cdot n \ .$$

Dirac magnetic monopoles are highly ionizing due to the large value of g. They are accelerated by the magnetic field, causing relativistically stretched parabolic trajectories. Because of the unique signature from monopoles, it is possible to effectively eliminate background while maintaining high efficiency. By demonstrating monopole consistent behavior throughout the detector, we expect that a single observed event could be compellingly claimed a discovery.

The CDF detector consists of a magnetic spectrometer including silicon and drift chamber tracking detectors and a scintillator time-of-flight system, surrounded by central and forward electromagnetic and hardronic calorimeter and muon detectors. The important detector components for this search are the central outer tracker (COT), and the time-of-flight (TOF) detector. The coverage of the cylindrical COT extends out to $|\eta| \sim 1$, where η is the pseudorapidity defined by $\eta = -\log \tan \theta$ and θ is the polar angle with respect to the proton beam direction. The COT consists of eight superlayers, each containing 12 layers of sense wires, alternating between stereo and axial superlayers from the center outward. The COT is surrounded by the TOF scintillator bars, which run parallel to the beam pipe and are instrumented on both ends by photomultiplier tubes (PMTs) [13].

II. DATA SAMPLE

The search uses 25 pb^{-1} of data collected by the CDF detector during 2003, in proton-antiproton collisions at $\sqrt{s} = 1.96$ TeV produced by the Fermilab Tevatron. The luminosity measurement has a 6% uncertainty. The data is collected using a specialized magnetic monopole trigger, described in Section III.

III. THE MAGNETIC MONOPOLE TRIGGER

The main feature of this search is the highly efficient dedicated monopole trigger, which requires large light pulses from both ends of a TOF scintillator bar. Due to their large ionization and massive production of delta rays, monopoles in scintillator with $\beta > 0.2$ are expected to produce light in excess of 500 MIPs. This is a tiny fraction of their overall energy loss, but it still represents a robust signal [5, 6]. Understanding the efficiency of the trigger is central to this analysis. The electronics response of the TOF has been thoroughly calibrated, and the trigger thresholds at ~ 30 MIPs are well below the expected response to a monopole, and have a neglible effect on the efficiency.

No other particle mimics the parabolic trajectory of a monopole, so the TOF acceptance must be estimated from Monte Carlo, which requires modifications to GEANT. Our implementation treats monopoles with the same care as electrically charged particles, including the acceleration from the magnetic field, energy loss and multiple scattering.

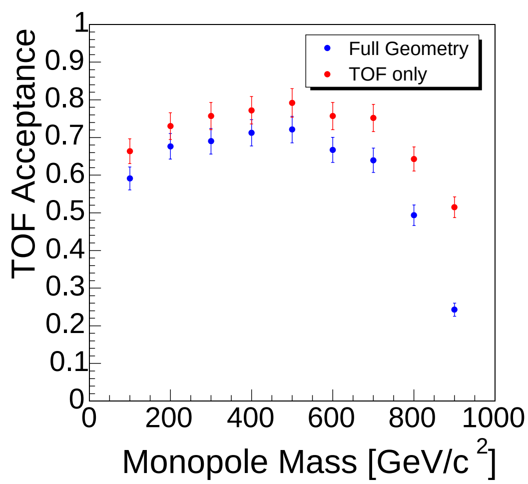

FIG. 1: The acceptance of the TOF for monopoles.

Figure 1 shows the TOF acceptance for Drell-Yan monopole pairs using GEANT. Light monopoles, accelerated severely by the magnetic field, tend to be swept out along the beam-pipe. Heavy monopoles, produced near threshold with limited kinetic energy and small p_t, suffer the same fate.

Figure 1 also compares a full simulation of the detector with a fictitious configuration consisting solely of the TOF. The material in the detector lowers the acceptance, due to energy loss and multiple scattering, but is a small correction to the main effect of the magnetic field. The main systematic uncertainty to the acceptance is due to the monopole's interaction with material, which cannot be validated on data. We assign a systematic error of 1/2 the total estimated effect: 4%.

Because the TOF electronics make a single measurement for each photomultiplier tube (PMT) for each event, tracks arriving early in the TOF bar, called spoilers, can effectively screen later arriving monopoles. This effect is mitigated by the long charge integration window of $\sim 20\ ns$ for this data set.

To measure the effect in data, we use $Z \to e^+e^-$ events, which have an underlying event similar to monopole pair production. The high p_t electrons also mimic the $r - \phi$ non-curvature of monopoles, meaning that we can check for

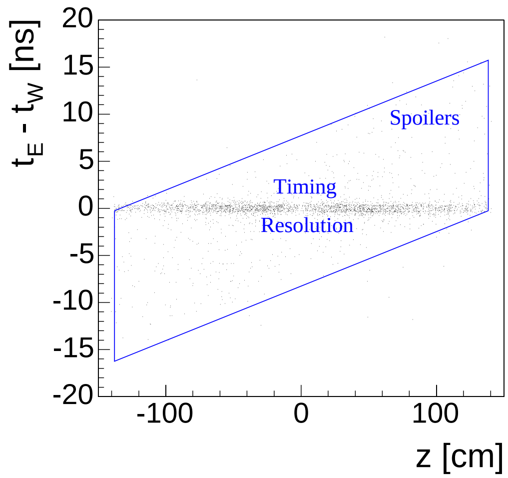

FIG. 2: The east minus west arrival time measurement versus track z position.

the presence of spoilers in the electron bars to estimate the effect for monopoles. For events with spoilers, the time difference between the two PMT pulses—the east and west—will be inconsistent with the z position of the track.

The difference between the east and west arrival time measurements versus z is shown in Figure 2. Consistent events form the central band, with the width determined by the timing resolution. Spoilers form the parallelogram with sides equal to the optical length of the bars. The shape comes from the vanishing phase space for spoiler to hit between a track and a PMT as the track gets close to the PMT. A likelihood fit including resolution and spoiler contributions measures the spoiler fraction at 14%.

The dependence of the spoiler fraction on luminosity contributes a systematic error. Because the underlying event from $Z \to e^+e^-$ may be different from monopole pair production, we also measure the dependence on the summed p_t of all tracks in the event. Finally, our fit doesn't completely disentangle resolution effects from spoiler effects, due to broad shoulders in the resolution function. To estimate this systematic uncertainty from this effect, we fix the broad gaussian in the resolution function to 500 ns and refit. We assign a systematic uncertainty of 5% from all of these effects.

Because monopoles are massive, they can have slow velocities, and arrive at the TOF too late to cause a trigger. Since the trigger requires a coincidence from both the east and the west PMTs, some pulses must travel the whole distance of the bar, taking 20 ns. The latest pulses from 900 GeV monopoles can arrive as late as 70 ns after the interaction, which is outside the TOF timing window's upper edge at 54 ns. The efficiency of the latest pulse to reach the PMT within the timing window has been measured with Monte Carlo. Only heavy monopoles move slowly enough to be effected; and then only slighly. A 900 GeV monopole is out of time in 10% of events. This is a negligible effect on lighter monopoles.

IV. MONOPOLE CANDIDATE SELECTION

CDF's 1.4 T solenoidal magnetic field is parallel to the proton beam direction, which is taken as the z direction, with ϕ the azimuthal angle, and r the radial distance. Monopoles curve in the $r - z$ plane, in sharp contrast to ordinary matter, which curves in the $r - \phi$ plane. In the COT, a monopole candidate combines abnormally high ionization with non-curvature in $r - \phi$, which requires modifications to the standard track reconstruction.

The COT measures the time interval for which the current on a sense wire is above a threshold, which is an indirect measurement of the amount of ionization from the passing particle. This measurement, called the hit width and measured in nanoseconds, is the offline measurement of ionization used for monopole candidate selection. An extrapolation of the COT response for ordinary tracks predicts monopoles would produce hit widths of about 232 ns. Although this is still within the dynamic range of the electronics, we do not cut at this level. Instead, we cut at 140 ns, in the tail of the distribution from ordinary matter, but far below the expected response from a monopole. As a result, this width cut has a negligible effect on the efficiency.

The default COT tracking algorithm first reconstructs small track segments in the COT's eight superlayers. It

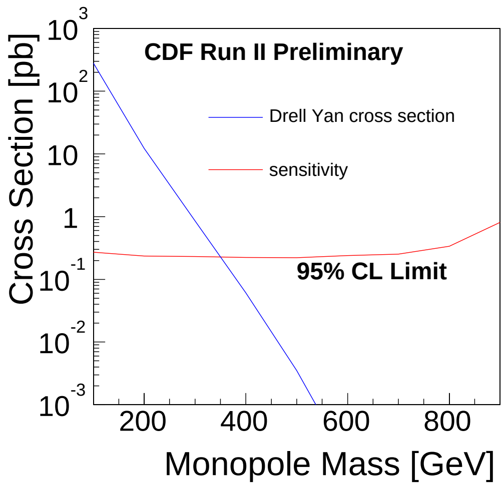

FIG. 3: Cross section sensitivity versus magnetic monopole mass. The excluded region is above.

Effect	Efficiency	Statistical Uncertainty	Systematic Uncertainty
TOF acceptance (MC)	Figure 1	Figure 1	4%
TOF response	100%	negl.	negl.
TOF spoilers	86%	1%	5%
TOF timing (MC)	$> 95\%$ for $m \leq 800$ GeV	5%	2.5%
COT width cut	100%	negl.	negl.
COT segment finding	94%	5%	3%

TABLE I: Summary of efficiency.

checks for "seeds" of three nearby hits, and then extends the seeds by checking for additional hit times consistent with a straight line fit. Because this is a rough fit, the timing tolerance is 20 ns.

In the monopole algorithm, the segments are required to be composed entirely of high dE/dx hits as described above. Also, because a monopole can have a slow and changing transverse velocity, the usual timing assumption ($t_{\text{flight}} = r/c$) cannot be used. Instead, the time-of-flight to each superlayer is allowed to vary.

A monopole candidate consists of several ϕ coincident low curvature segments. From Monte Carlo, we choose a loose curvature cut at < 0.001. Likewise, the ϕ tolerance is a loose 0.2 radians. The remaining cuts are on the minimum number of hits allowed in a segment, and on the total number of ϕ coincident segments required for a monopole candidate. By ignoring the width cut, the segment finding algorithm efficiency can be measured using high p_t tracks. In this manner, we choose a highly efficient cut requiring 7 coincident superlayers with at least 8 hits in each segment. This has a 94% efficiency with a 5% statistical uncertainty.

As a cross check, we measure the algorithm's efficiency on monopoles, and find that the Monte Carlo is optimistic; the offline algorithm has nearly 100% efficiency on Monte Carlo. One half the difference between the Monte Carlo and data is taken as a systematic error (3%).

To estimate how effectivly these cuts reject background, we use minimum bias data. For a minimum number of 7 hits, there are a few events of 800 thousand with a two-fold coincidence. We require a seven-fold coincidence of 8 hits or more.

V. RESULTS

No events in this data sample pass the monopole candidate requirements, and we report a limit. Monopole production limits are typically reported by the cross section sensitivity as a function of monopole mass, to minimize the dependence on a particular production model. The expected number of events N from a process with cross section σ and detector efficiency ϵ after integrated luminosity L is given by:

$$N = L\epsilon\sigma \ .$$

A cross section sensitivity is thus given by

$$\sigma^* = N^*/L\epsilon \ .$$

Using baysian statistics, N^* absorbs the fractional uncertainty in the total acceptance. For a 95% CL limit with .1 fractional uncertainty on the acceptance, $N^* = 3.084$.

Our exclusion limit is shown in Figure 3 based on the efficiency, as summarized in Table I. For the Drell-Yan like mechanism, this implies a mass limit of $m > 350$ GeV. This mass limit is well within the range of high efficiency for this search, meaning that additional data will significantly improve the limit.

[1] P.A.M. Dirac, *Quantized Singularities In The Electromagnetic Field*, Proc. R. Soc. (London), A133 (1931).

[2] Searches for cosmic flux of magnetic monopoles:
I. De Mitri, *Search For Magnetic Monopoles in the Cosmic Radiation with the Macro Detector at Gran Sasso*, Budapest 2001, High energy physics, hep2001/213.
S. Cecchini et al., *Search for Magnetic Monopoles at the Chacaltaya Cosmic Ray Laboratory*, Nuovo Cim.24C:639-644 (2001).
S.D. Wick, T.W. Kephart, T.J. Weiler, P.L. Biermann, *Signatures for a Cosmic Flux of Magnetic Monopoles*, astro-ph/0001233 (2000).

[3] Searches for effects of virtual magnetic monopoles:
I.F. Ginzburg, A. Schiller, *Search For a Heavy Magnetic Monopole at the Tevatron and LHC*, Phys.Rev.D57:6599-6603 (1998), HEP-PH 9802310.
B. Abbot et al, *A Search for Heavy Pointlike Dirac Monopoles*, Fermilab-Pub-98/095-E (1998).
M. Acciarri et al., *Search for Anomalous $Z \to \gamma\gamma\gamma$ Events at Lep*, Phys. Lett. B345, 609-616 (1995).
There are some difficulties with virtual searches:
L. Gamberg, G.R. Kalbfleisch, K.A. Milton, *Direct and Indirect Searches for Low-Mass Magnetic Monopoles*, hep-ph/9906526, (1999).

[4] A search for monopoles trapped in detector material:
G.R. Kalbfleisch, W. Luo, K.A. Milton, E.H. Smith, M.G. Strauss, *Limits on Production of Magnetic Monopoles Utilizing Samples from the D0 and CDF Detectors at the Tevatron*, hep-ex/0306045.

[5] A summary of magnetic monopole searches:
G. Giacomelli, L. Patrizii, *Magnetic Monopole Searches*, Trieste 2002, Astroparticle physics and cosmology 121-144, hep-ex/0302011.

[6] hep-ex/0302011
hep-ex/0207020

[7] Theory of monopole production and scattering cross sections:
J. Schwinger, K.A. Milton, W. Tsai, L.L. DeRaad, D.C. Clark, *Nonrelativistic Dyon-Dyon Scattering*, Ann. Phys. (N.Y.) 101, 451 (1976)
L. Gamberg, K.A. Milton, *Dual quantum electrodynamics: Dyon-dyon and charge-monopole scattering in a high-energy approximation*, Phys. Rev. D 61, (2000).
L. Gamberg, K.A. Milton, *Eikonal scattering of monopoles and dyons in dual QED*, OKHEP-00-05, (2000).

[8] Particle Data Group, Eur. Phys. J. C3, 144 (1998).

[9] J.D. Jackson, *Classical Electrodynamics*, Second Edition. New York: de Gruyter, (1982).

[10] J. Schwinger, L.L. DeRaad Jr., K.A. Milton, W. Tsai, *Classical Electrodynamics*, Reading, MA: Perseus Books, (1998).
M.E. Peskin, D.V. Schroeder, *An Introduction to Quantum Field Theory*, Reading, MA: Perseus Books, (1995).
W. Greiner, J. Rafelski, *Spezielle Relativitätstheorie*, 3. überarb. Auflage. Frankfurt: Harri Deutsch, (1992).

[11] W.H. Press, B.P. Flannery, S.A. Teukolsky, W.T. Vetterling, *Numerical Recipes in Pascal*, Cambridge University Press, (1989).

[12] *GEANT Detector Description and Simulation Tool*, CERN Program Library Writeup W5013, (1994).

[13] F. Abe, et al., Nucl. Instrum. Methods Phys. Res. A **271**, 387 (1988); D. Amidei, et al., Nucl. Instum. Methods Phys. Res. A **350**, 73 (1994); F. Abe, et al., Phys. Rev. D **52**, 4784 (1995); P. Azzi, et al., Nucl. Instrum. Methods Phys. Res. A **360**, 137 (1995); The CDFII Detector Technical Design Report, Fermilab-Pub-96/390-E

[14] Torbjoern Sjoestrand, *Pythia 5.7 and Jetset 7.4 Physics and Manual*, (1998).